Nuclear structure in ^{132}Sn region with new generation RIBs

Angela Gargano

INFN Napoli

L. Coraggio (Napoli)
A. Covello (Napoli)
N. Itaco (Napoli)
T.T.S. Kuo (Stony Brook)

Element	A	Z	N	T1/2 s	RIBs 260keV 1+	Re-accelerated RIBs	q+	Max E/A	
In	114	49	65	7.19E+01	4,61E+05	9,22E+03	20	12	SIS+LIS so
In	115	49	66	1.39E+22	4,23E+06	8,46E+04	20	12	
In	116	49	67	1.41E+01	7,38E+06	1,48E+05	20	12	
In	117	49	68	2.59E+03	8,29E+07	1,66E+06	20	11,8	
In	118	49	69	5.00E+00	5,35E+07	1,07E+06	20	11,6	
In	119	49	70	1.44E+02	5,88E+08	1,18E+07	20	11,4	
In	120	49	71	3.08E+00	2,27E+08	4,54E+06	20	11,4	
In	121	49	72	2.31E+01	1,32E+09	2,64E+07	20	11,4	
In	122	49	73	1.50E+00	3,51E+08	7,02E+06	20	11,2	
In	123	49	74	5.98E+00	1,08E+09	2,16E+07	20	11,2	
In	124	49	75	3.11E+00	6,67E+08	1,33E+07	20	11,2	
In	125	49	76	2.36E+00	4,25E+08	8,50E+06	20	11	
In	126	49	77	1.60E+00	2,00E+08	4,00E+06	20	11	
In	127	49	78	1.09E+00	7,58E+07	1,52E+06	20	11	
In	128	49	79	8.40E-01	2,53E+07	5,07E+05	20	11	
In	129	49	80	6.10E-01	5,44E+06	1,09E+05	20	10,9	
In	130	49	81	3.20E-01	7,72E+05	1,54E+04	20	10,9	
In	131	49	82	2.82E-01	1,38E+05	2,76E+03	20	10,9	
In	132	49	83	2.01E-01	9,89E+04	1,98E+03			
In	133	49	84	1.80E-01	1,02E+04				
Sn	121	50	71	9.74E+04	2,02E+09	4,04E+07	21	12.0	LIS source
Sn	123	50	73	1.12E+07	1,28E+10	2,56E+08	21	11.9	
Sn	125	50	75	8.33E+05	3,50E+10	7,00E+08	21	11.7	
Sn	126	50	76	3.16E+12	4,21E+10	8,42E+08	21	11.7	
Sn	127	50	77	7.56E+03	4,08E+10	8,16E+08	21	11.7	
Sn	128	50	78	3.54E+03	3,18E+10	6,36E+08	21	11.7	
Sn	129	50	79	1.34E+02	1,75E+10	3,50E+08	21	11.6	
Sn	130	50	80	2.23E+02	7,89E+09	1,58E+08	21	11.5	
Sn	131	50	81	5.60E+01	3,42E+09	6,83E+07	21	11.5	
Sn	132	50	82	3.97E+01	1,56E+09	3,11E+07	21	11.4	
Sn	133	50	83	1.45E+00	1,38E+08	2,76E+06	21	11.3	
Sn	134	50	84	1.12E+00	2,49E+07	4,99E+05	21	11.0	
Sn	135	50	85	2.50E-01	3,11E+05	6,21E+03	21	11.0	
Sn	136	50	86	9.20E-02	4,99E+03				
Sb	119	51	68	1.37E+05	1,50E+05	3,00E+03	21	12.0	LIS source
Sb	120	51	69	9.53E+02	8,21E+05	1,64E+04	21	12.0	
Sb	122	51	71	2.35E+05	4,35E+07	8,70E+05	21	11.9	
Sb	124	51	73	5.20E+06	6,87E+08	1,37E+07	21	11.8	
Sb	125	51	74	8.70E+07	1,98E+09	3,96E+07	21	11.7	
Sb	126	51	75	1.08E+06	4,53E+09	9,06E+07	21	11.7	
Sb	127	51	76	3.33E+05	8,37E+09	1,67E+08	21	11.7	
Sb	128	51	77	3.24E+04	1,19E+10	2,38E+08	21	11.7	
Sb	129	51	78	1.58E+04	1,39E+10	2,78E+08	21	11.6	
Sb	130	51	79	2.37E+03	1,03E+10	2,06E+08	21	11.5	
Sb	131	51	80	1.38E+03	6,06E+09	1,21E+08	21	11.5	

Element	A	Z	N	T1/2 s	RIBs 260keV 1+	Re-accelerated RIBs	q+	Max E/A
Sb	132	51	81	1.67E+02	1,90E+09	3,80E+07	21	11.5
Sb	133	51	82	1.50E+02	8,06E+08	1,61E+07	21	11.0
Sb	134	51	83	7.80E+01	3,09E+07	6,19E+05	21	11.0
Sb	135	51	84	1.71E+00	1,44E+07	2,88E+05	21	10.7
Sb	136	51	85	8.20E-01	2,06E+06	4,12E+04	21	10.7
Sb	137	51	86	2.06E-01	1,48E+05	2,97E+03	21	10.6
Sb	138	51	87	2.26E-01	1,84E+04			
Te	127	52	75	3.37E+04	1,75E+09	3,50E+07	21	11.7
Te	128	52	76	6.94E+31	6,24E+09	1,25E+08	21	11.7
Te	129	52	77	4.18E+03	1,05E+10	2,10E+08	21	11.6
Te	130	52	78	2.49E+28	3,22E+10	6,44E+08	21	11.5
Te	131	52	79	1.50E+03	2,37E+10	4,74E+08	21	11.5
Te	132	52	80	2.77E+05	4,21E+10	8,42E+08	21	11.5
Te	133	52	81	7.50E+02	1,56E+10	3,13E+08	21	11.0
Te	134	52	82	2.51E+03	1,17E+10	2,33E+08	21	11.0
Te	135	52	83	1.90E+01	1,37E+09	2,73E+07	21	10.7
Te	136	52	84	1.75E+01	5,48E+08	1,10E+07	21	10.7
Te	137	52	85	2.49E+00	8,39E+07	1,68E+06	21	10.6
Te	138	52	86	1.40E+00	2,15E+07	4,30E+05	21	10.0
Te	139	52	87	3.51E-01	2,16E+06	4,32E+04	22	11.0
Te	140	52	88	2.46E-01	2,76E+05	5,51E+03	22	10.9
Te	141	52	89	2.65E-01	1,77E+03			
I	125	53	72	5.13E+06	2,15E+06	4,30E+04	21	11.7
I	126	53	73	1.13E+06	1,83E+07	3,66E+05	21	11.7
I	128	53	75	1.50E+03	3,11E+08	6,22E+06	21	11.7
I	129	53	76	4.95E+14	4,19E+09	8,38E+07	21	11.6
I	130	53	77	4.45E+04	1,62E+10	3,24E+08	21	11.5
I	131	53	78	6.93E+05	5,47E+10	1,09E+09	21	11.5
I	132	53	79	8.26E+03	9,15E+10	1,83E+09	21	11.5
I	133	53	80	7.49E+04	1,89E+11	3,78E+09	21	11.0
I	134	53	81	3.15E+03	1,36E+11	2,72E+09	21	11.0
I	135	53	82	2.37E+04	1,73E+11	3,46E+09	21	10.7
I	136	53	83	8.34E+01	1,04E+10	2,08E+08	21	10.7
I	137	53	84	2.45E+01	2,18E+09	4,37E+07	21	10.6
I	138	53	85	6.49E+00	3,44E+08	6,89E+06	21	10.0
I	139	53	86	2.29E+00	5,94E+07	1,19E+06	22	11.0
I	140	53	87	8.60E-01	9,17E+06	1,83E+05	22	10.9
I	141	53	88	4.30E-01	1,40E+06	2,80E+04	22	10.7
I	142	53	89	2.00E-01	1,22E+05	2,44E+03	22	10.7
I	143	53	90	2.78E-01	1,24E+04	2,49E+02	22	11.5
Xe	127	54	73	3.14E+06	3,11E+04	6,22E+02	21	11.7
Xe	133	54	79	4.53E+05	4,71E+09	9,42E+07	21	11.3
Xe	135	54	81	3.29E+04	1,96E+10	3,92E+08	21	11.0
Xe	137	54	83	2.29E+02	9,86E+09	1,97E+08	21	10.7
Xe	138	54	84	8.45E+02	1,01E+10	2,02E+08	21	10.6
Xe	139	54	85	3.97E+01	2,15E+09	4,30E+07	21	10.5
Xe	140	54	86	1.36E+01	6,72E+08	1,34E+07	21	10.0
Xe	141	54	87	1.73E+00	1,19E+08	2,38E+06	22	11.0
Xe	142	54	88	1.22E+00	3,74E+07	7,49E+05	22	10.9
Xe	143	54	89	3.00E-01	5,34E+06	1,07E+05	22	10.7

Outline

- Some examples of recent experiments in ^{132}Sn region

- Nuclei in ^{132}Sn region within the realistic shell-model approach
  - **Theoretical framework**
  - **Some results in the perspective of new generation RIBs**

- Summary

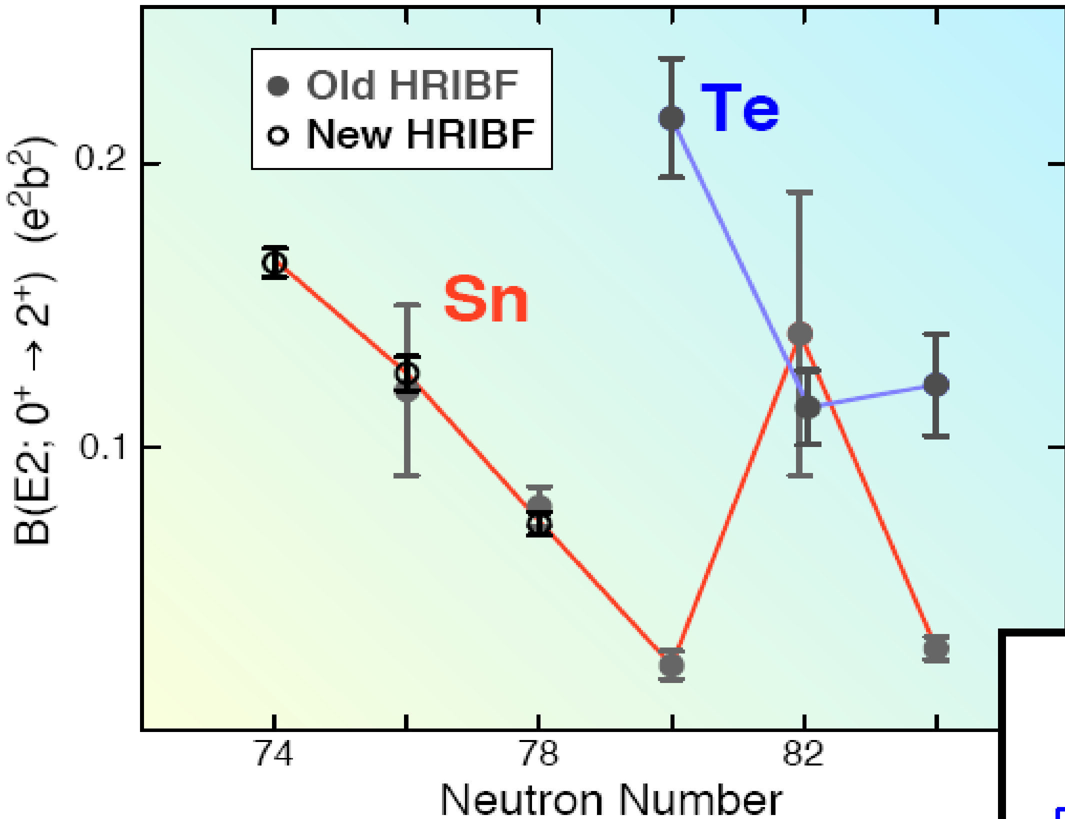

Coulex @HRIBF

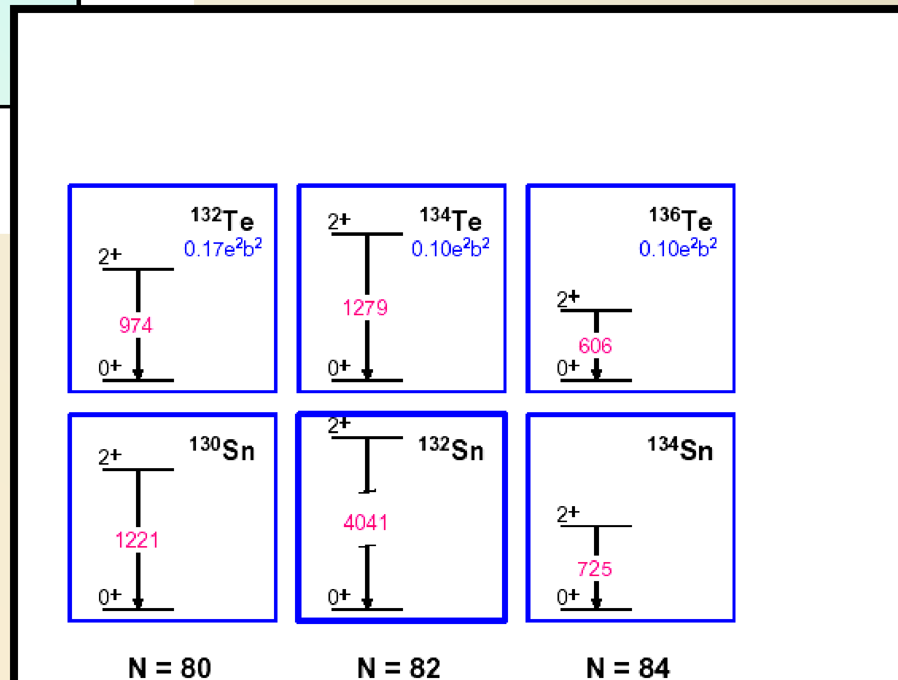

B(E2) values are lower than expected from

Grodzins-Raman Scaling:
Product of B(E2; 0 -> 2) . E(2$^+$)
~ [2.6 * Z^2/ A$^{2/3}$]

From J.R. Beene et al. J. Phys. G to be published

Evolution of the one-phonon $2^+_{1,ms}$ mixed-symmetry state in $N=80$ isotones as a local measure for the proton–neutron quadrupole interaction

T. Ahn [a,b,c,*], L. Coquard [c], N. Pietralla [c], G. Rainovski [d], A. Costin [b], R.V.F. Janssens [e], C.J. Lister [e], M. Carpenter [e], S. Zhu [e], K. Heyde [f]

Physics Letters B 679 (2009) 19

An inverse kinematics Coulomb excitation experiment was performed to obtain absolute $E2$ and $M1$ transition strengths in ^{134}Xe. The measured transition strengths indicate that the 2^+_3 state of ^{134}Xe is the dominant fragment of the one-phonon $2^+_{1,ms}$ mixed-symmetry state. Comparing the energy of the $2^+_{1,ms}$ mixed-symmetry state in ^{134}Xe to that of the $2^+_{1,ms}$ levels in the $N=80$ isotonic chain indicates that the separation in energy between the fully-symmetric 2^+_1 state and the $2^+_{1,ms}$ level increases as a function of the number of proton pairs outside the $Z=50$ shell closure. This behavior can be understood as resulting from the mixing of the basic components of a two-fluid quantum system. A phenomenological fit based on this concept was performed. It provides the first experimental estimate of the strength of the proton–neutron quadrupole interaction derived from nuclear collective states with symmetric and antisymmetric nature.

@Argonnne NL

^{12}C(^{134}Xe, ^{134}Xe*)
E/A 3.2 MeV

E_{level} (keV)	J^π	τ (ps)	E_γ (keV)	J^π_{final}	I_γ	A_2/A_0	A_4/A_0	δ	$B(E2)$ (W.u.)	$B(M1)$ (μ_N^2)
847	2^+_1	3.0(2)[a]	847	0^+_1	1000(9)	0.119(7)	−0.006(9)		15.3(11)[a]	
1614	2^+_2	1.9(1)	767	2^+_1	4.70(5)	−0.262(8)	−0.01(1)	−1.5(2)	20(2)	0.015(1)
			1614	0^+_1	4.93(8)	0.28(1)	−0.06(2)		0.74(5)	
1731	4^+_1	3.2(2)[a]	884	2^+_1	1.79(2)				11.6(8)[a]	
1920	3^+_1		1073	2^+_1	0.355(5)			0.16(2)[a]		
1947	2^+_3	0.23(2)	1100	2^+_1	3.44(4)	0.27(1)	0.01(1)	0.08(2)	0.56(4)	0.30(2)
			1947	0^+_1	0.515(9)	0.306[b]	−0.074[b]		0.72(7)	
2116	(4)		1269	2^+_1						
2263	2^+_4	0.54(4)	1415	2^+_1	0.73(1)	0.33(2)	0.07(2)	0.14(2) 1.6(1)	0.14(1)[c] 5.6(4)[d]	0.041(3)[c] 0.012(1)[d]
			2263	0^+_1	0.63(1)	0.322[b]	−0.091[b]		0.63(6)	
2867	(0–4)		921	2^+_3	0.25(4)					
			1254	2^+_2	0.35(6)					
			2020	2^+_1	0.38(6)					

PRL 100, 072501 (2008) PHYSICAL REVIEW LETTERS week ending 22 FEBRUARY 2008

Restoration of the $N = 82$ Shell Gap from Direct Mass Measurements of ^{132,134}Sn

M. Dworschak,[1,*] G. Audi,[2] K. Blaum,[1,3,4] P. Delahaye,[5] S. George,[1,3] U. Hager,[6] F. Herfurth,[1] A. Herlert,[5] A. Kellerbauer,[4] H.-J. Kluge,[1,7] D. Lunney,[2] L. Schweikhard,[8] and C. Yazidjian[1]

A high-precision direct Penning trap mass measurement has revealed a 0.5-MeV deviation of the binding energy of ^{134}Sn from the currently accepted value. The corrected mass assignment of this neutron-rich nuclide restores the neutron-shell gap at $N = 82$, previously considered to be a case of "shell quenching." In fact, the new shell gap value for the short-lived ^{132}Sn is larger than that of the doubly magic ^{48}Ca which is stable. The $N = 82$ shell gap has considerable impact on fission recycling during the r process. More generally, the new finding has important consequences for microscopic mean-field theories which systematically deviate from the measured binding energies of closed-shell nuclides.

@ ISOLDE - CERN

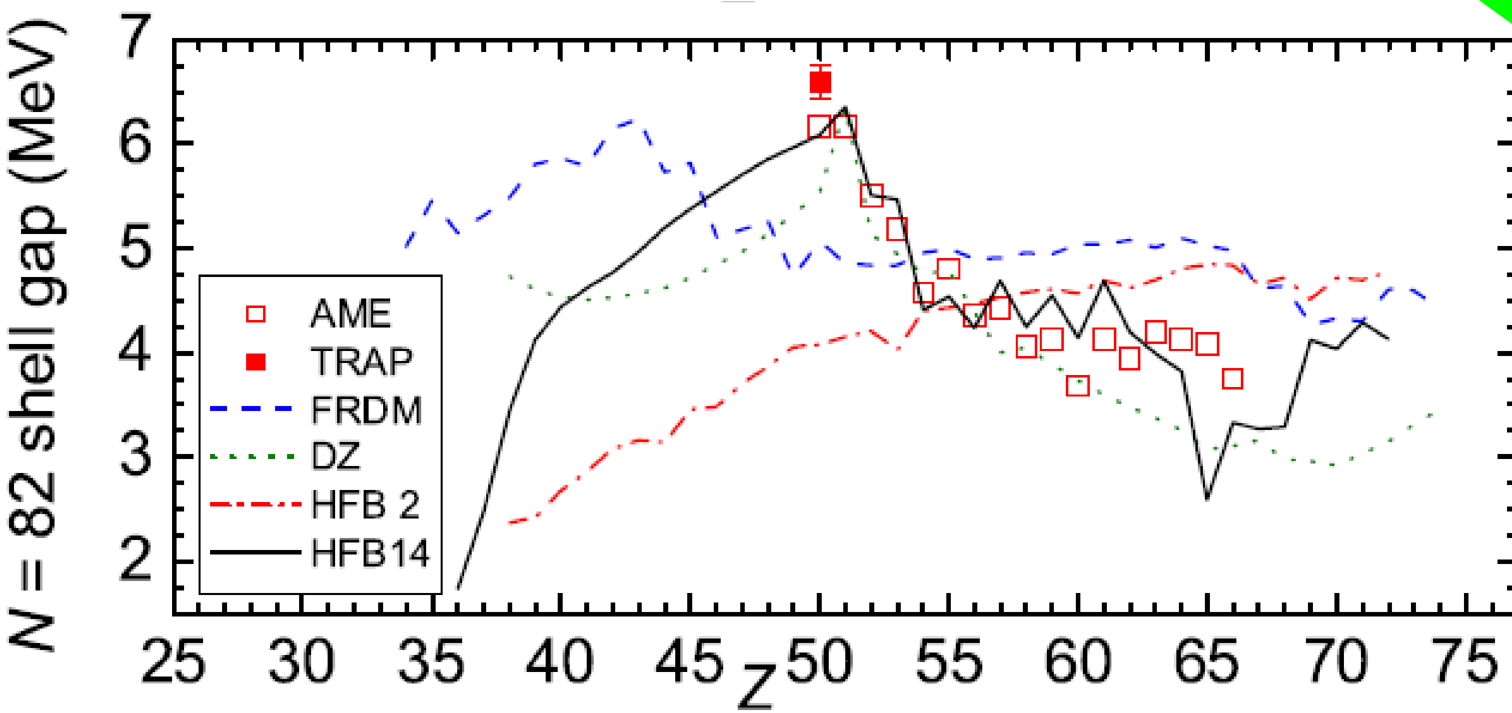

nature
Vol 465| 27 May 2010| doi:10.1038/nature09048

The magic nature of ^{132}Sn explored through the single-particle states of ^{133}Sn

K. L. Jones[1,2], A. S. Adekola[3], D. W. Bardayan[4], J. C. Blackmon[4], K. Y. Chae[1], K. A. Chipps[5], J. A. Cizewski[2], L. Erikson[5], C. Harlin[6], R. Hatarik[2], R. Kapler[1], R. L. Kozub[7], J. F. Liang[4], R. Livesay[5], Z. Ma[1], B. H. Moazen[1], C. D. Nesaraja[4], F. M. Nunes[8], S. D. Pain[2], N. P. Patterson[6], D. Shapira[4], J. F. Shriner Jr[7], M. S. Smith[4], T. P. Swan[2,6] & J. S. Thomas[6]

@ HRIBF –Oak Ridge

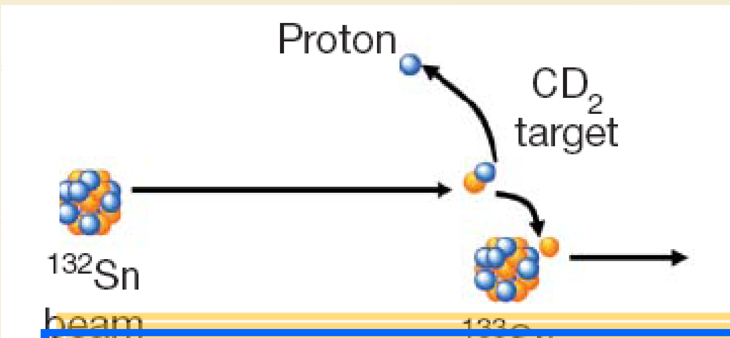

Table 1 | Properties of the four single-particle states populated by the ^{132}Sn(d,p)^{133}Sn reaction

E_x (keV)	J^{π}	Configuration	S	C^2 (fm^{-1})
0	$7/2^-$	$^{132}\mathrm{Sn}_{gs} \otimes \nu_{f7/2}$	0.86 ± 0.16	0.64 ± 0.10
854	$3/2^-$	$^{132}\mathrm{Sn}_{gs} \otimes \nu_{p3/2}$	0.92 ± 0.18	5.61 ± 0.86
$1,363 \pm 31$	$(1/2^-)$	$^{132}\mathrm{Sn}_{gs} \otimes \nu_{p1/2}$	1.1 ± 0.3	2.63 ± 0.43
2,005	$(5/2^-)$	$^{132}\mathrm{Sn}_{gs} \otimes \nu_{f5/2}$	1.1 ± 0.2	$(9 \pm 2) \times 10^{-4}$

Shell-model calculations

$$H = \sum_i \varepsilon_i a_i^+ a_i + \frac{1}{4}\sum_{ijkl} \langle ij | V | kl \rangle a_i^+ a_j^+ a_l a_k$$

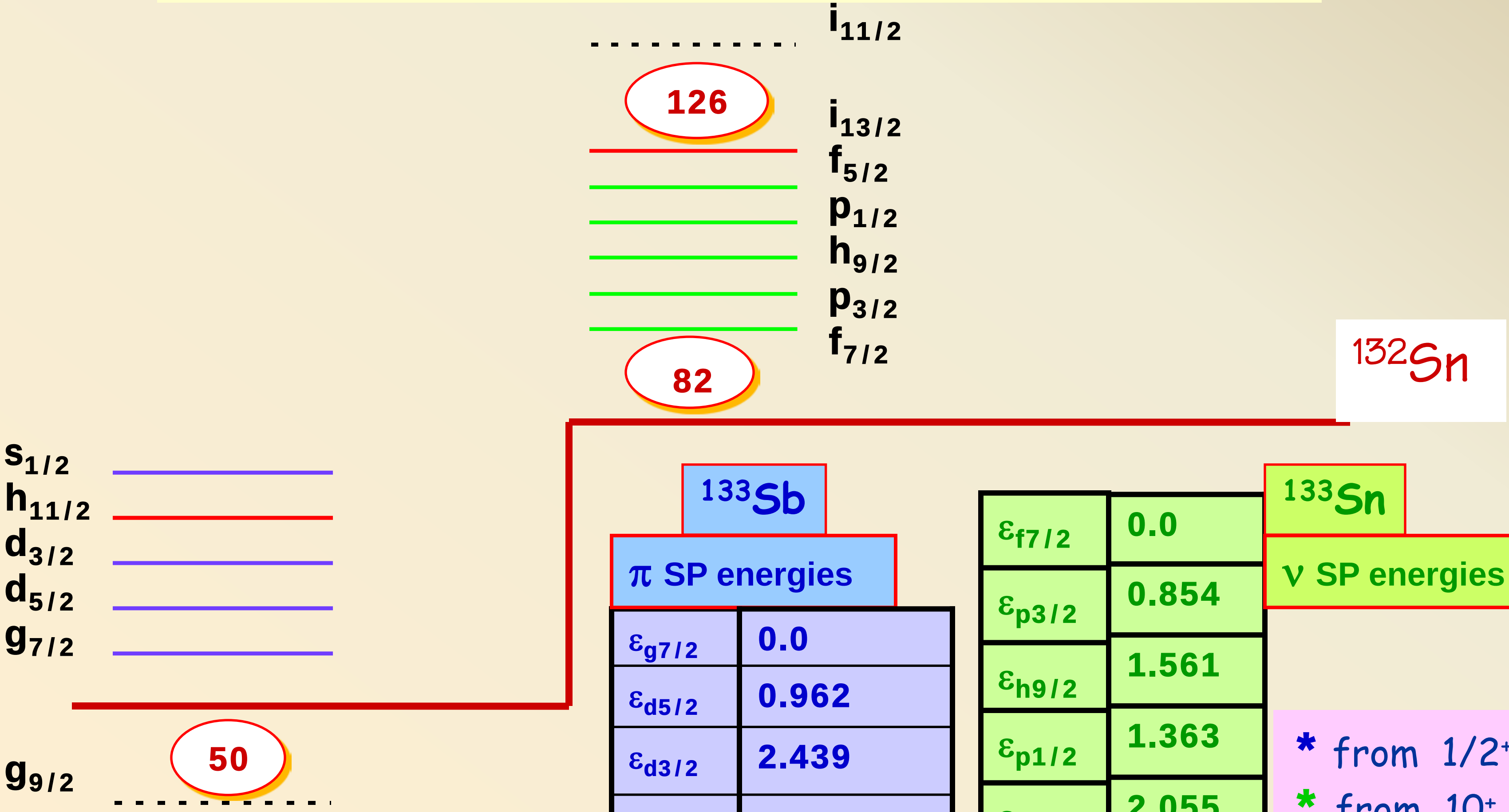

^{133}Sb

π SP energies

$\varepsilon_{g7/2}$	0.0
$\varepsilon_{d5/2}$	0.962
$\varepsilon_{d3/2}$	2.439
$\varepsilon_{s1/2}$	2.800*
$\varepsilon_{h11/2}$	2.793

^{133}Sn

ν SP energies

$\varepsilon_{f7/2}$	0.0
$\varepsilon_{p3/2}$	0.854
$\varepsilon_{h9/2}$	1.561
$\varepsilon_{p1/2}$	1.363
$\varepsilon_{f5/2}$	2.055
$\varepsilon_{i13/2}$	2.694*

* from 1/2$^+$ in ^{139}La
* from 10$^+$ in ^{134}Sb

- **Choice of the nucleon-nucleon potential**

CD-Bonn, Argonne V_{18} , Chiral potentials,…

all modern NN potentials fit equally well the deuteron properties and the NN scattering data up the inelastic threshold

$\chi^2/N_{data} \sim 1$

these potentials cannot be used directly in the derivation of V_{eff} due to their strong short-range repulsion, but a

- **Renormalization procedure is needed**

Renormalization of the *NN* interaction

V_{low-k} approach: construction of a low-momentum *NN* potential V_{low-k} confined within a momentum-space cutoff $k \leq <$

Derived from the original V_{NN} by integrating out the high-momentum components of the original V_{NN} potential down to the cutoff momentum Λ

V_{low-k} decouples high- and low-energy degrees of freedom

preserves the physics of the original NN interaction

- the deuteron binding energy
- scattering phase-shifts up to the cutoff momentum Λ

S. Bogner,T.T.S. Kuo,L. Coraggio,A. Covello,N. Itaco, Phys. Rev C 65, 051301(R) (2002)
S. Bogner, T.T.S. Kuo, A. Schwenk, Phys. Rep. 386, 1 (2003)
L. Coraggio et al, Prog. Part. Nucl. Phys. 62 (2009) 135

Two-body effective interaction

$\hat{Q}$-box + folded diagram method

developed within the framework of the time-dependent perturbative approach by Kuo and co-workers

$$V_{eff} = \hat{Q} + \sum_{i=1}^{\infty} F_i$$

$\hat{Q}$-box

collection of irreducible valence-linked diagrams with $V_{low\text{-}k}$ replacing V_{NN} in the interaction vertices

Diagramatic expression of the $\hat{Q}$-box

F ... lo ... s of $\hat{Q}$-box derivatives)

1-body diagrams up to 2nd order

S-box

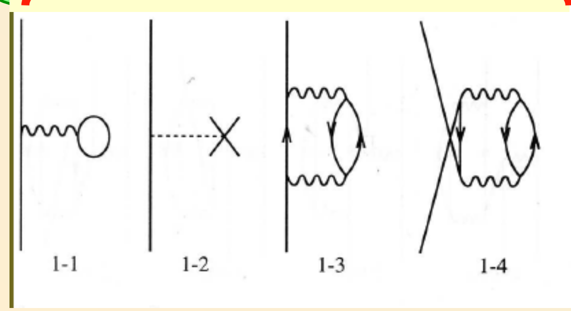

+

2-body diagrams up to 2nd order:

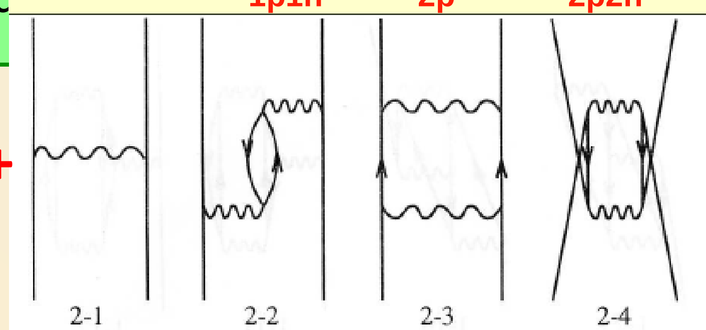

+ ...

... Nucl. Phys. 62 (2009) 135

A realistic effective interaction

is constructed for two valence particles

is defined

-in the nuclear medium

-in a subspace of the Hilbert space

➔ accounts perturbatively for

- configurations excluded from the chosen model space
- excitations of the core nucleons

Results

- Binding energies
- Excitation energies and angular momenta
- Electromagnetic properties
- Single particle properties

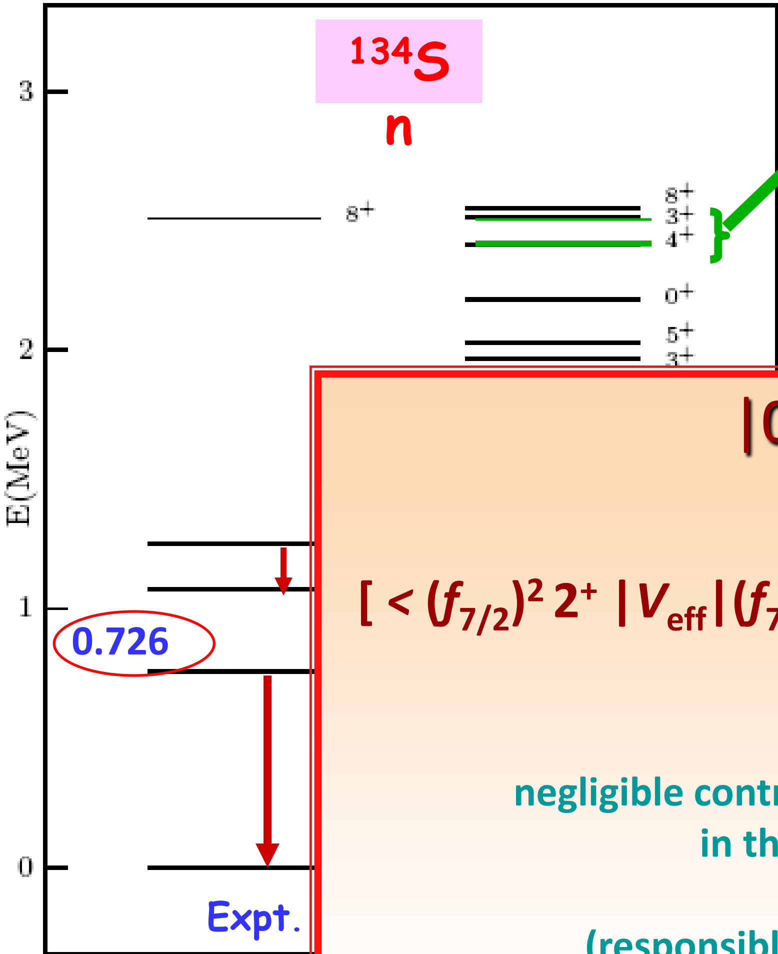

from the $f_{7/2}p_{1/2}$ configuration
their location below the 8^+
due to the new position of the
$p_{1/2}$ level measured @ ORNL
$\varepsilon_{p1/2}$=1.36 MeV
(old value: 1.66 MeV)
[Nature 465 (2010)]

$|0^+, g.s>, |2^+_1> \sim (f7/2)^2$ ➦
small $0^+ - 2^+$ spacing ➦

$[< (f_{7/2})^2\, 2^+ \,|V_{eff}|\, (f_{7/2})^2\, 2^+ > - < (f_{7/2})^2\, 0^+ \,|V_{eff}|\, (f_{7/2})^2\, 0^+ >] \sim 0.4$ MeV

⬇

negligible contribution of the one particle-one hole excitations
in the effective interaction of two neutrons
above the *N* = 82 shell,
(responsible for the increase of pairing below this shell)

E(3^-) in ^{132}Sn $\sim \Delta_n$ - 500 keV

^{134}Sn Coulex (Oak Ridge)

B(E2;$0^+ \rightarrow 2^+$) = 290(40) e^2fm^4

Theory

B(E2;$0^+ \rightarrow 2^+$) = 330 fm^4

e_{eff} (n)=0.70e
from B(E2;6→4)

Predictions for electromagnetic properties in ^{134}Sn

$B(E2;4_1 \rightarrow 2_1) = 67\ e^2fm^4$
$B(E2;2_2 \rightarrow 0) = 14\ e^2fm^4$
$B(E2;2_2 \rightarrow 2_1) = 118\ e^2fm^4$
$B(M1;2_2 \rightarrow 2_1) = 0.02\ \mu^2_N$

$Q(2_1) = -1.3\ efm^2$
$Q(2_2) = -2.8\ efm^2$
$\mu(2_1) = -0.56\ \mu_N$
$\mu(2_2) = -0.25\ \mu_N$

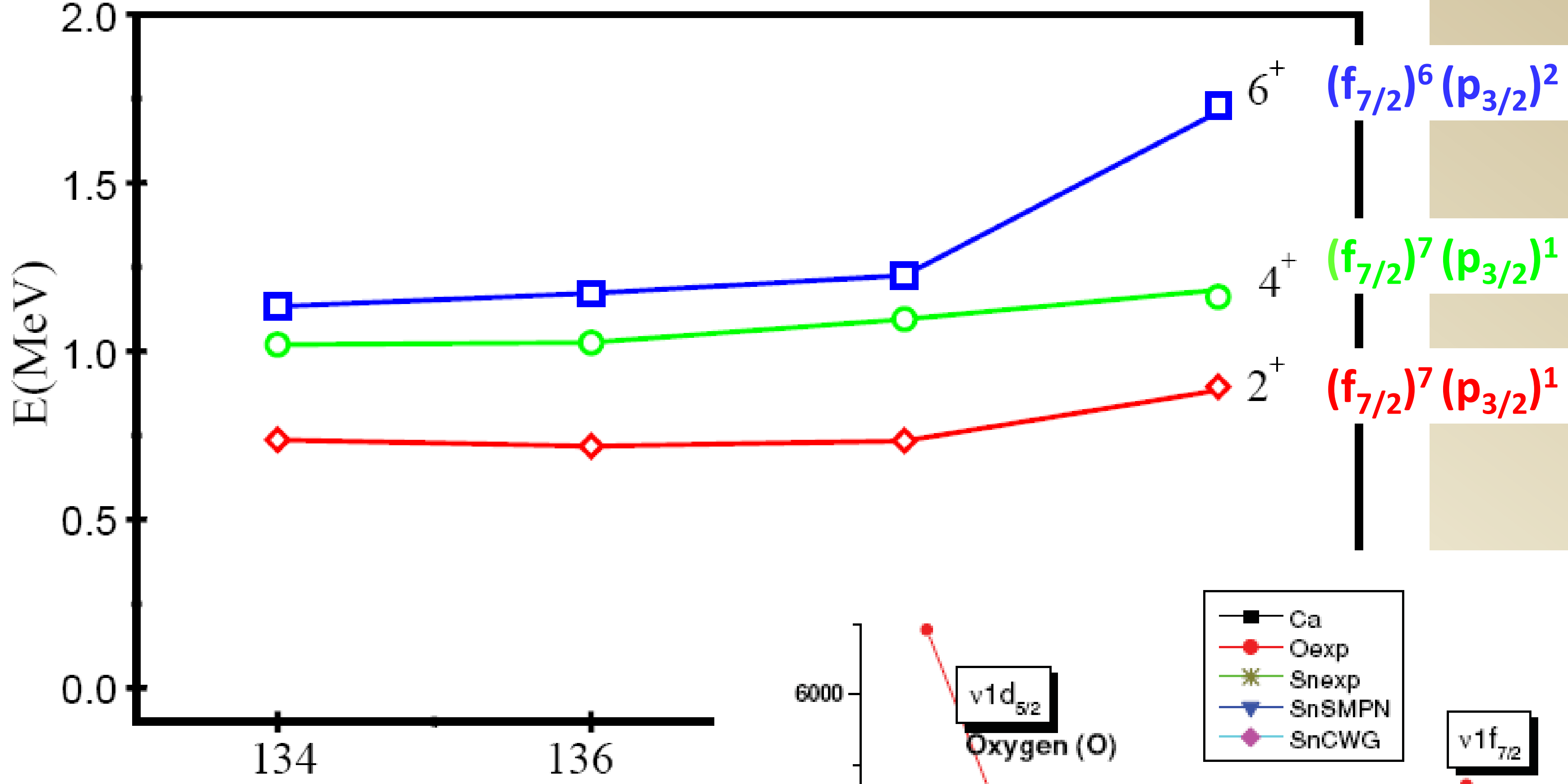

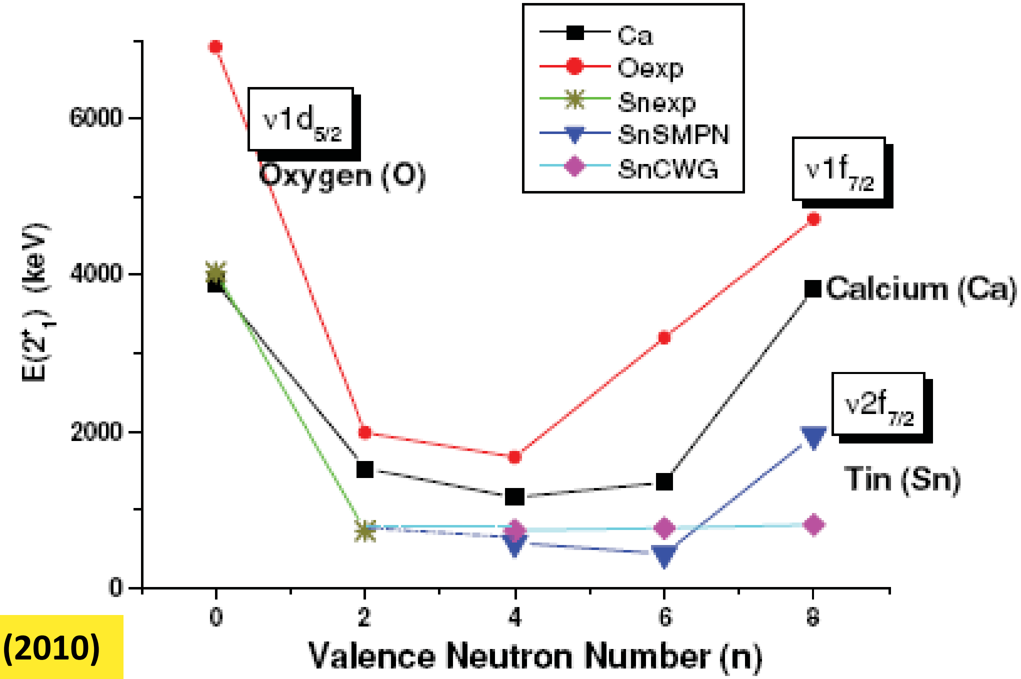

NO shell closure at *N* = 90

S. Sarkar and M. S. Sarkar Phys. Rev. C 81, 064328 (2010)

$$\mathrm{ESPE}(j) = \varepsilon_j + \sum_{j'} n_{j'} V_{jj'} \; ; \qquad V_{jj'} = \sum_J \frac{(2J+1)\langle jj'|V|jj'\rangle_J}{(2J+1)}$$

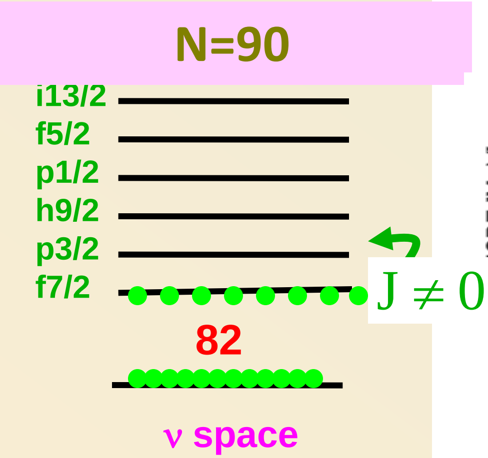

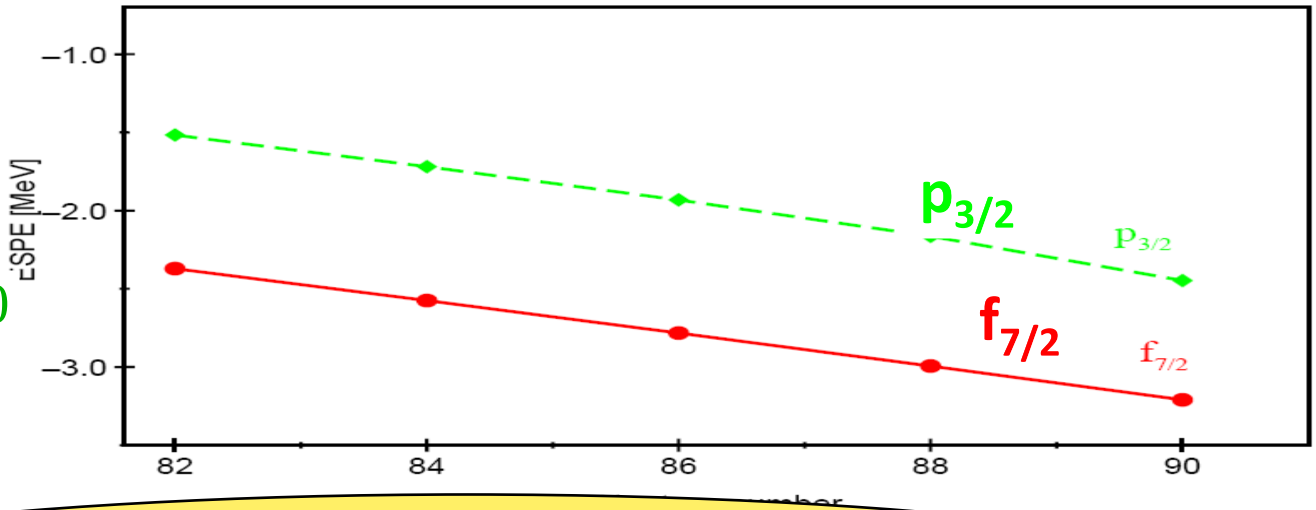

The energy difference between the two orbits remains almost constant and **even decreases slightly** by about 100 keV when moving from N = 82 to N = 90

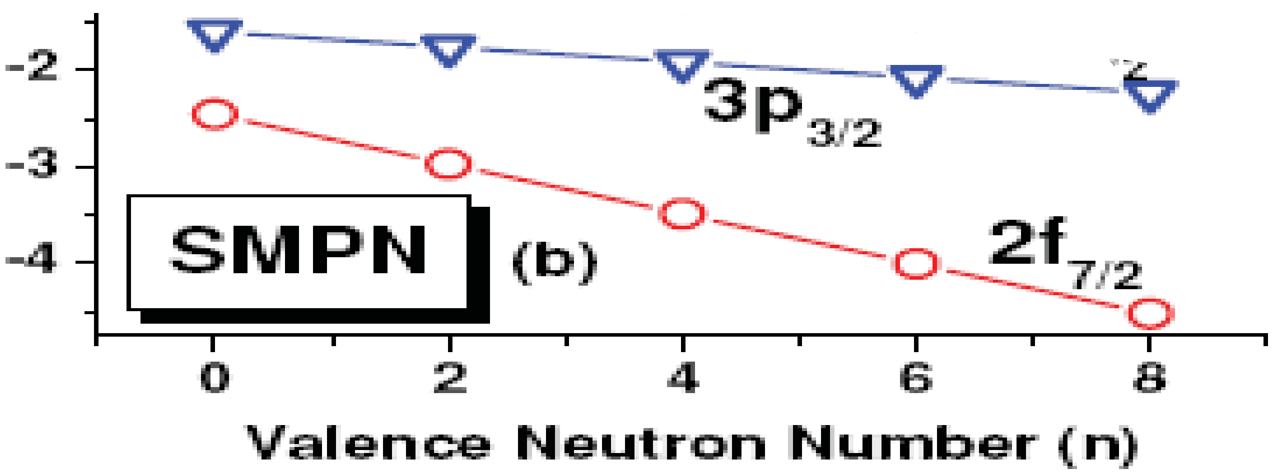

N/Z	1.68	1.72	1.76	1.80
A	^{134}Sn	^{136}Sn	^{138}Sn	^{140}Sn
BE Calc relative to ^{132}Sn	5.92	11.83	17.68	23.41
BE Expt relative to ^{132}Sn	5.916 ± 0.150*			
S_n Calc	3.55	3.55	3.53	3.50
S_n Expt	3.545 ± 0.152			

^{124}Sn(stable) with N/Z=1.48
BE/A=8.46

* M. Dworschak et al. Phys. Rev. Lett. 100, (2008) 072501
Old value (Fogelberg et al., 1999): 6.365 MeV
→neutron shell gap at N= 82 *restored*

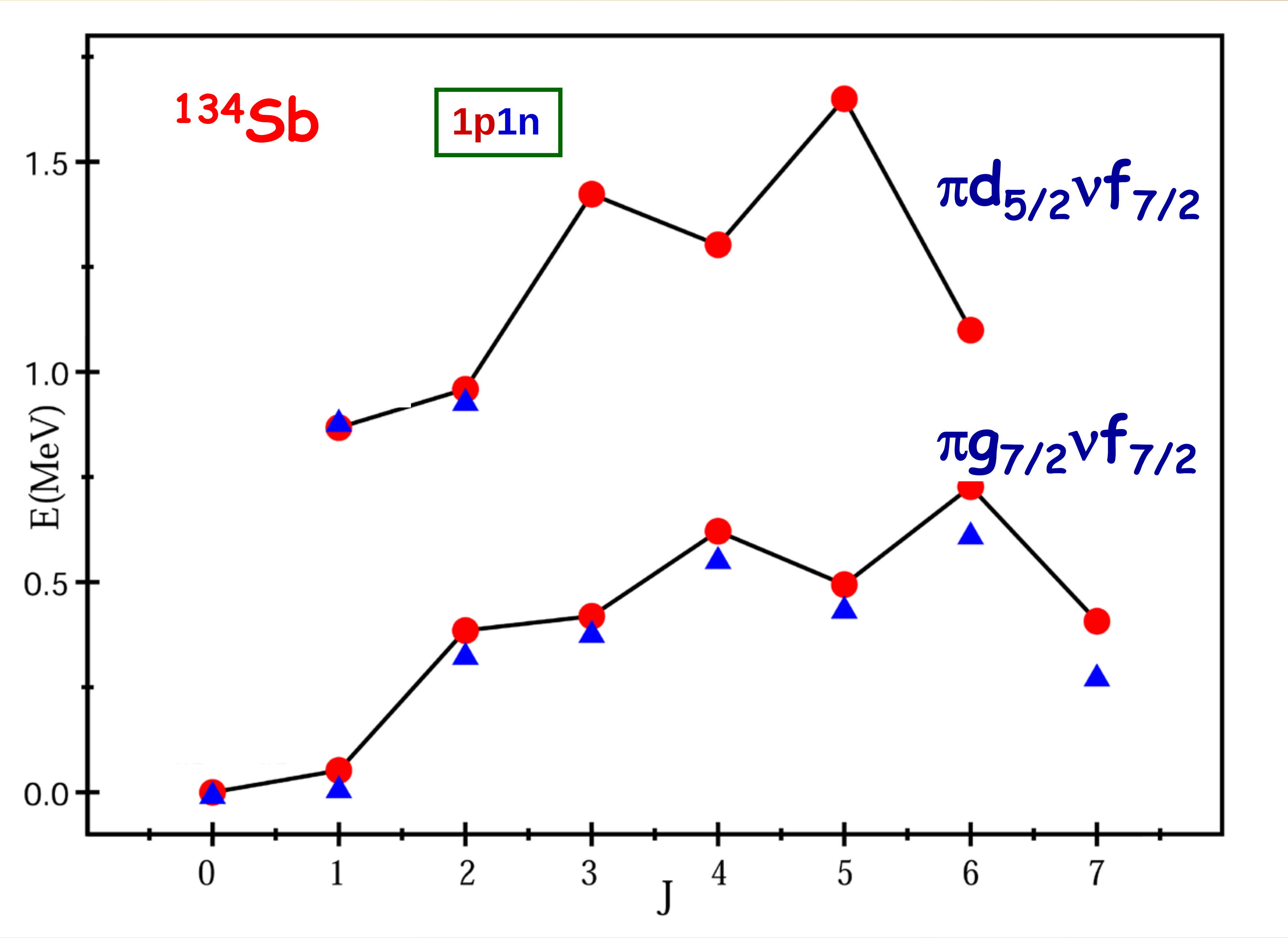

^{134}Sb
1p1n
$\pi d_{5/2} \nu f_{7/2}$
$\pi g_{7/2} \nu f_{7/2}$
E(MeV)
0.0
0.5
1.0
1.5
0
1
2
3
4
5
6
7
J

evolution of the "$\pi g_{7/2} \nu f_{7/2}$" multiplet

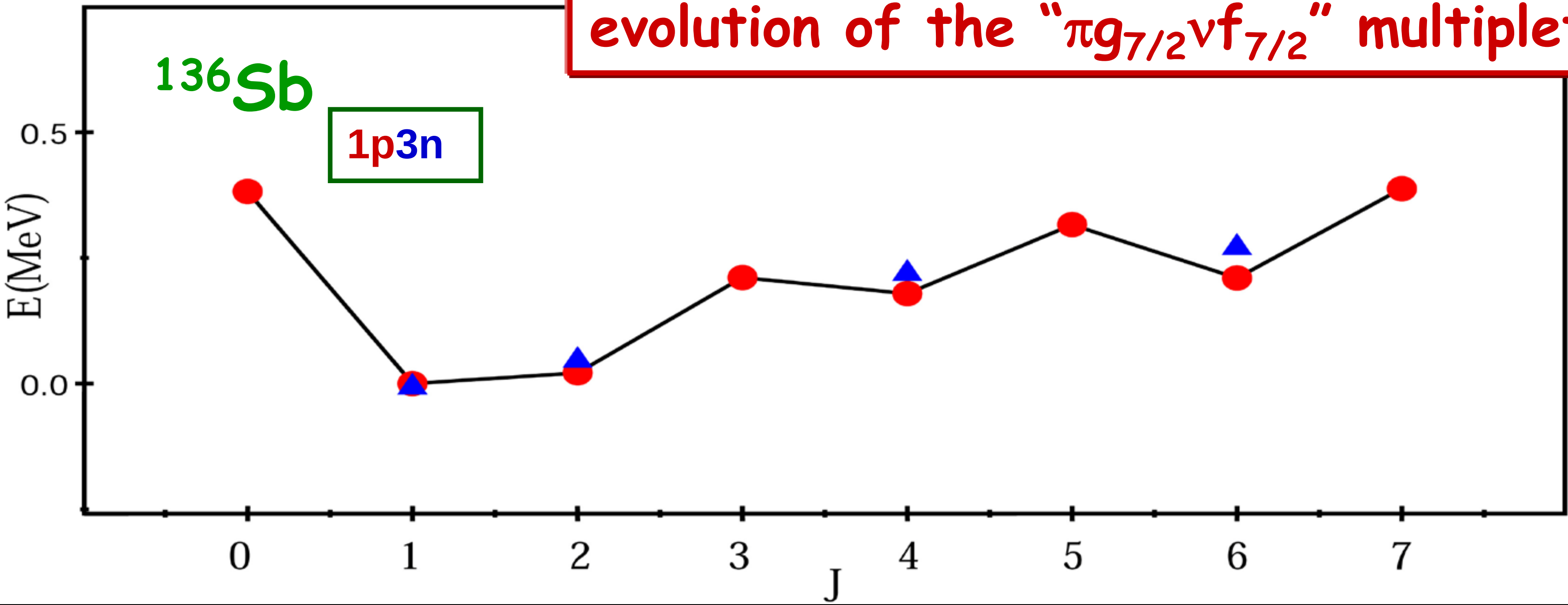

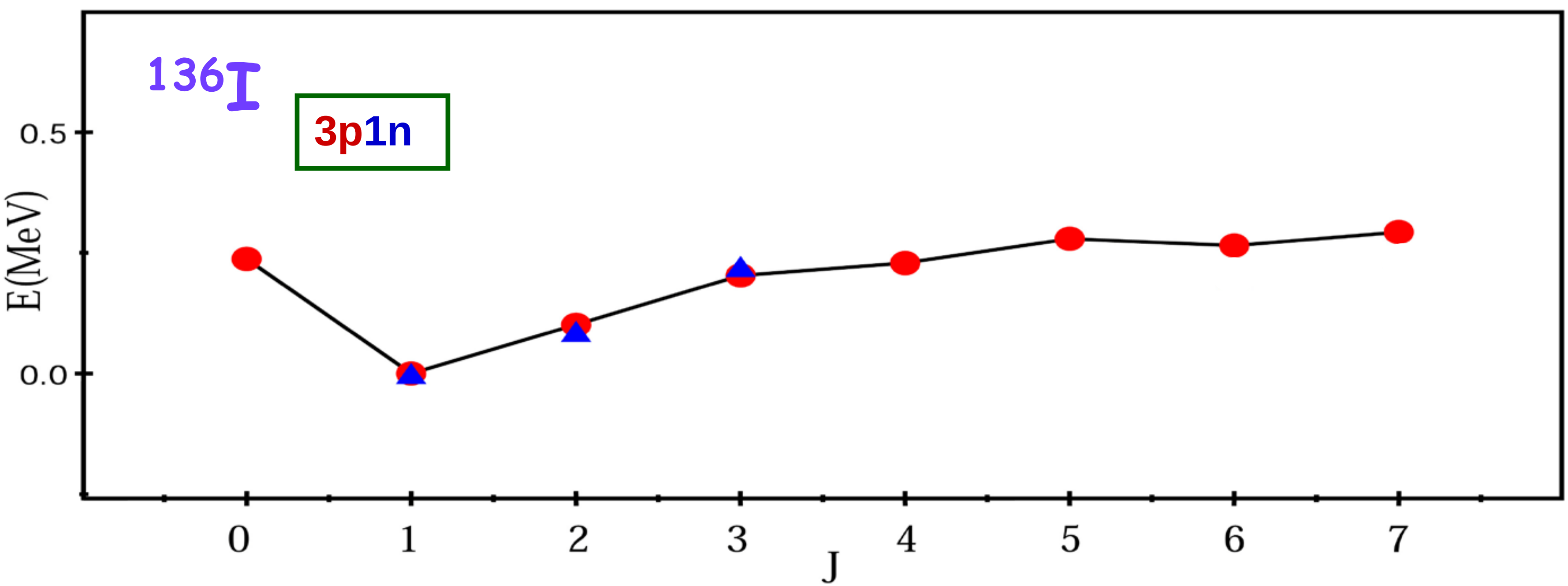

^{136}Te

^{132}Sn + 2ν +2π

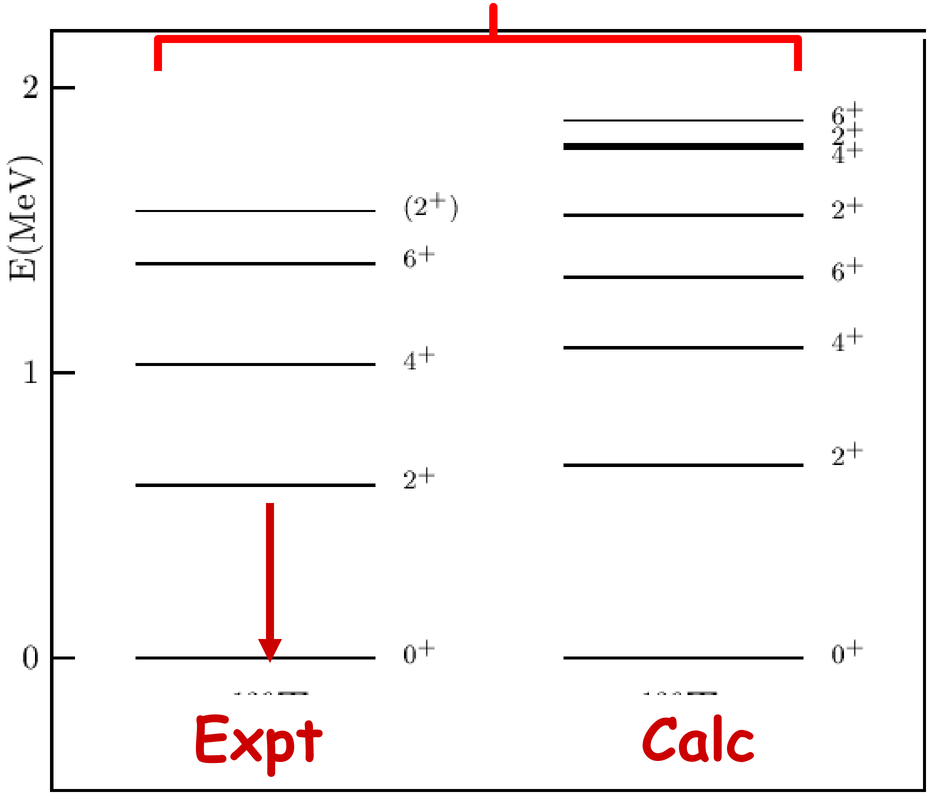

^{136}Te Coulex (Oak Ridge)

$B(E2;2^+ \rightarrow 0^+) = 206 \quad 33\ e^2fm^4$

New prelimary measurement ~300

Theory

$B(E2;0^+ \rightarrow 2^+) = 367\ e^2fm^4$

e_{eff} (π)=0.70e

e_{eff} (ν)=1.55e

Structure of the yrast states

$$|^{136}\mathrm{Te};\mathrm{g.s}\rangle = 0.85|^{134}\mathrm{Sn};\mathrm{g.s.}\rangle|^{134}\mathrm{Te};\mathrm{g.s.}\rangle + \cdots,$$

$$|^{136}\mathrm{Te};2_1^+\rangle = 0.73|^{134}\mathrm{Te};g.s.\rangle|^{134}\mathrm{Sn};2_1^+\rangle + 0.36|^{134}\mathrm{Sn};g.s.\rangle|^{134}\mathrm{Te};2_1^+\rangle + \cdots$$

$$|^{136}\mathrm{Te};4_1^+\rangle = 0.71|^{134}\mathrm{Te};g.s.\rangle|^{134}\mathrm{Sn};4_1^+\rangle + 0.28|^{134}\mathrm{Sn};g.s.\rangle|^{134}\mathrm{Te};|4_1^+\rangle + \cdots$$

$$|^{136}\mathrm{Te};6_1^+\rangle = 0.78|^{134}\mathrm{Te};g.s.\rangle|^{134}\mathrm{Sn};6_1^+\rangle - 0.21|^{134}\mathrm{Sn};g.s.\rangle|^{134}\mathrm{Te};6_1^+\rangle + \cdots$$

$B(E2;4_1 \rightarrow 2_1) = 460\ e^2fm^4$
$B(E2;6_1 \rightarrow 4_1) = 310\ e^2fm^4$

$Q(2_1) = -23\ efm^2$
$\mu(2_1) = 0.20\ \mu_N$

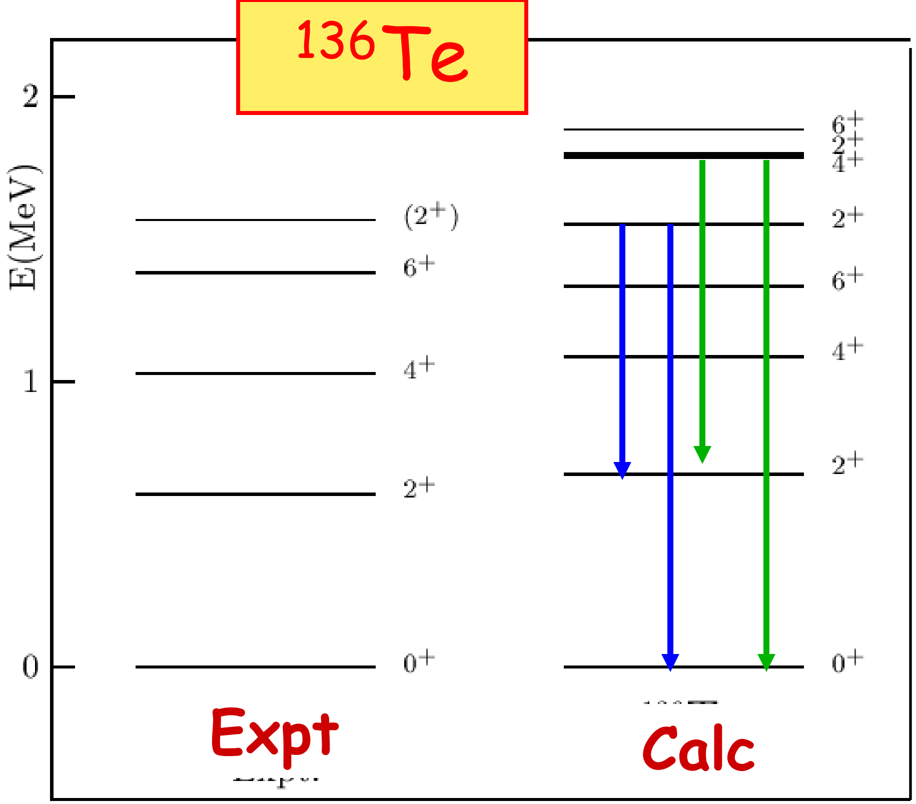

$B(E2;2_2 \rightarrow 0) = 24 \;\; e^2fm^4$

$B(E2;2_2 \rightarrow 2_1) = 360 \; e^2fm^4$

$B(M1;2_2 \rightarrow 2_1) = 0.18 \; \mu^2_N$

$B(E2;2_3 \rightarrow 0) = 34 \;\; e^2fm^4$

$B(E2;2_3 \rightarrow 2_1) = 50 \; e^2fm^4$

$B(M1;2_3 \rightarrow 2_1) = 0.19 \; \mu^2_N$

$$|{}^{136}\mathrm{Te};2_2^+\rangle = 0.61|{}^{134}\mathrm{Te};g.s.\rangle|{}^{134}\mathrm{Sn};2_2^+\rangle - 0.42|{}^{134}\mathrm{Te};g.s.\rangle|{}^{134}\mathrm{Sn};2_1^+\rangle + \cdots$$

$$|{}^{136}\mathrm{Te};2_3^+\rangle = 0.78|{}^{134}\mathrm{Sn};g.s.\rangle|{}^{134}\mathrm{Te};2_1^+\rangle - 0.31|{}^{134}\mathrm{Te};g.s.\rangle|{}^{134}\mathrm{Sn};2_1^+\rangle + \cdots$$

mixed-symmetry state (antisymmetric with respect to interchanges between proton and neutron pairs)

in IBM-2 $\left[\,|S_\nu \times D_\pi\rangle\right] - \left[\,|S_\pi \times D_\nu\rangle\right]/\sqrt{2}$

Evolution of the proton single-particle states

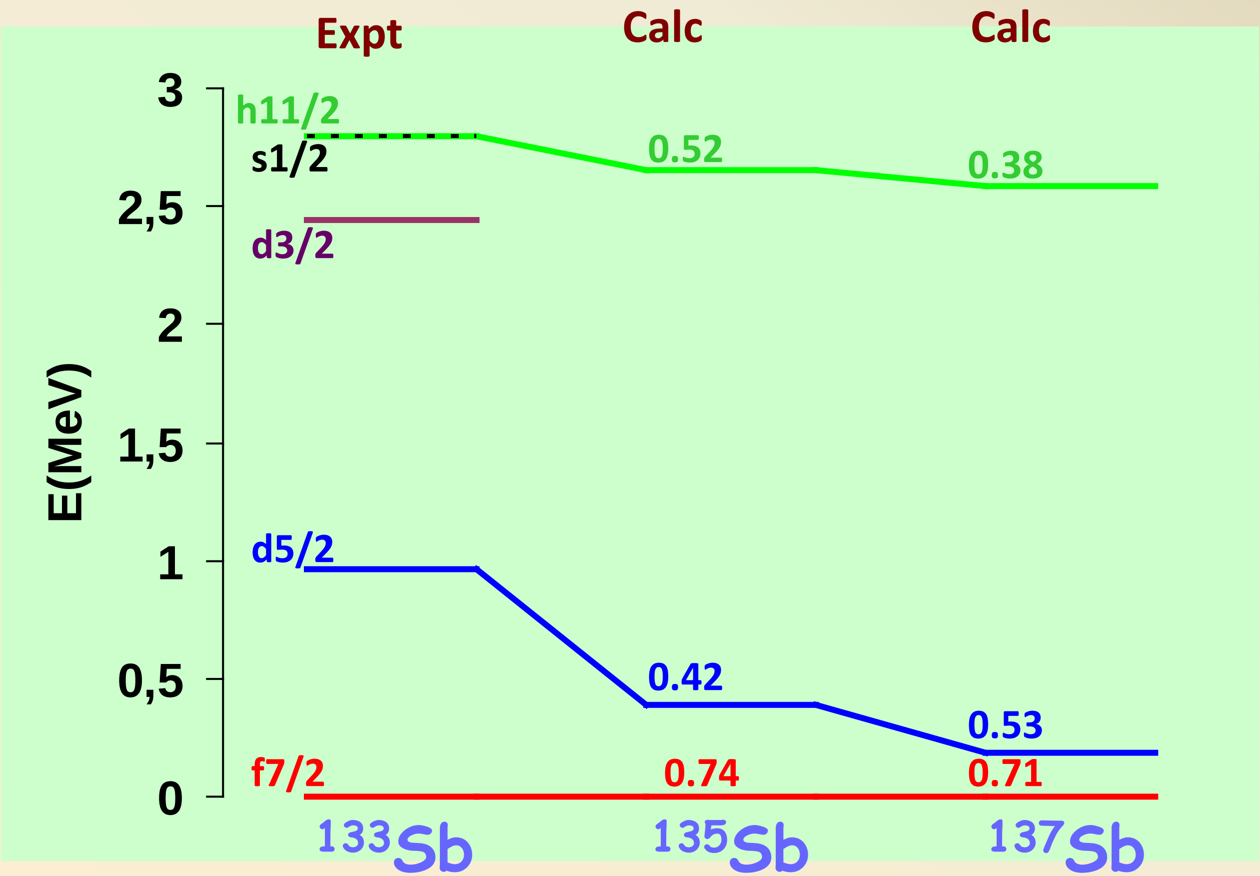

^{135}Sb		
J^{π}	Calc E(MeV)	Expt E(MeV)
$7/2^{+}$	0.0	0.0
$5/2^{+}$	0.391	0.282
$3/2^{+}$	0.509	0.440
$1/2^{+}$	0.678	0.573
$11/2^{+}$	0.750	0.707
$9/2^{+}$	0.813	0.798

$\pi d_{5/2}\ |\ ^{134}\mathrm{Sn, g.s.}>$
$\pi g_{7/2}\ |\ ^{134}\mathrm{Sn},\ 2_1^{+}>$

$d_{3/2}$ and $s_{1/2}$ single-particle strenght highly fragmented

^{135}Sb : Σ S(1/2)=0.29; Σ S(3/2)=0.25

^{137}Sb: Σ S(1/2)=0.24; Σ S(3/2)=0.16

(the sum includes states up to 2.8 MeV)

Evolution of the neutron single particle states

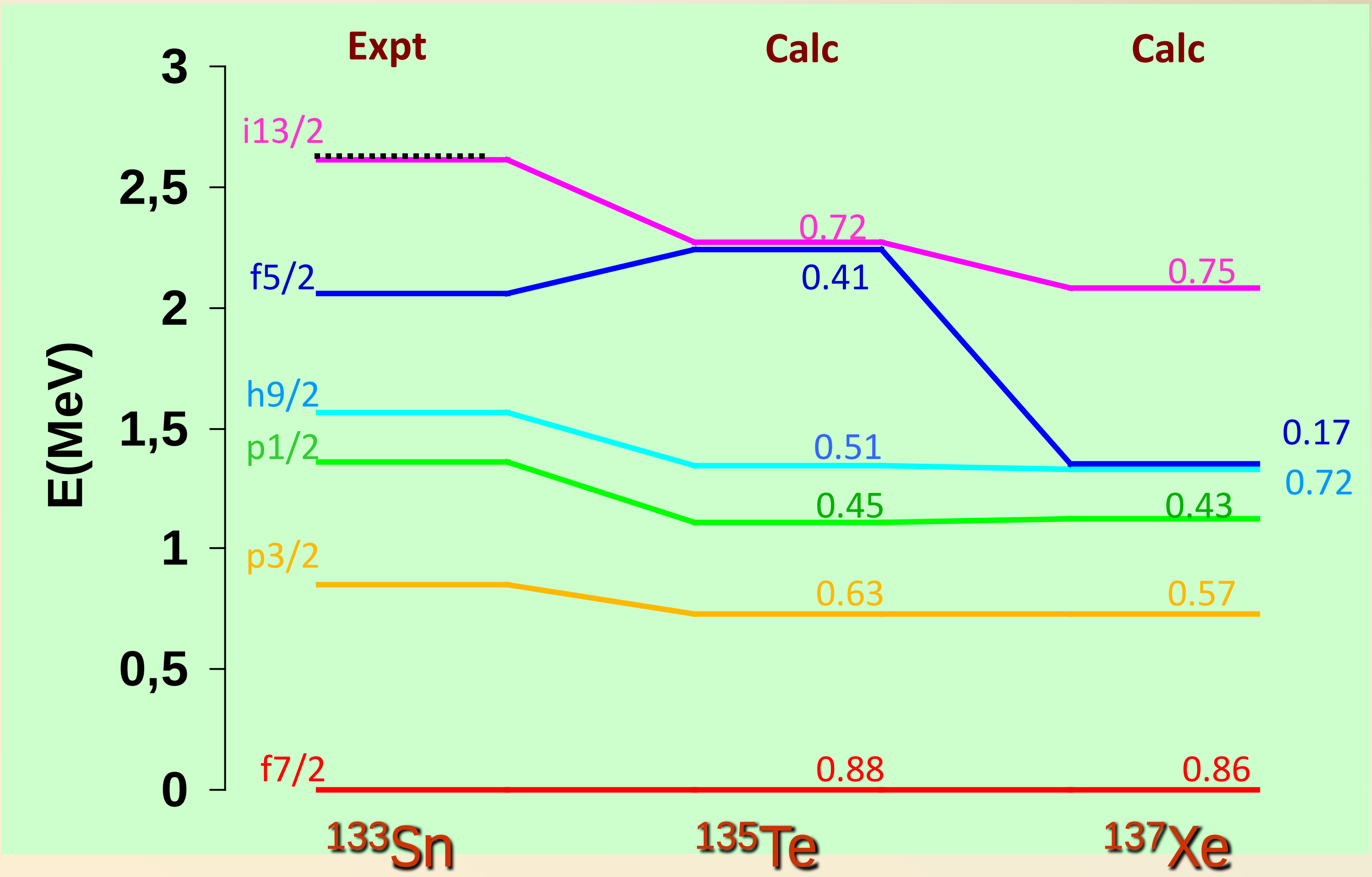

^{135}Te 5/2$^-$ and the 9/2$^-$ states with the largest single-particle strenght do not correspond to the yrast states $(5/2^-)_1$ ➔ E= 1.35 MeV S=0.12 $(9/2^-)_1$ ➔ E=1.302MeV S=0.18

J.A. Cizewski et al Newsletters @HRIBF

d(^{134}Te,p)^{135}Te

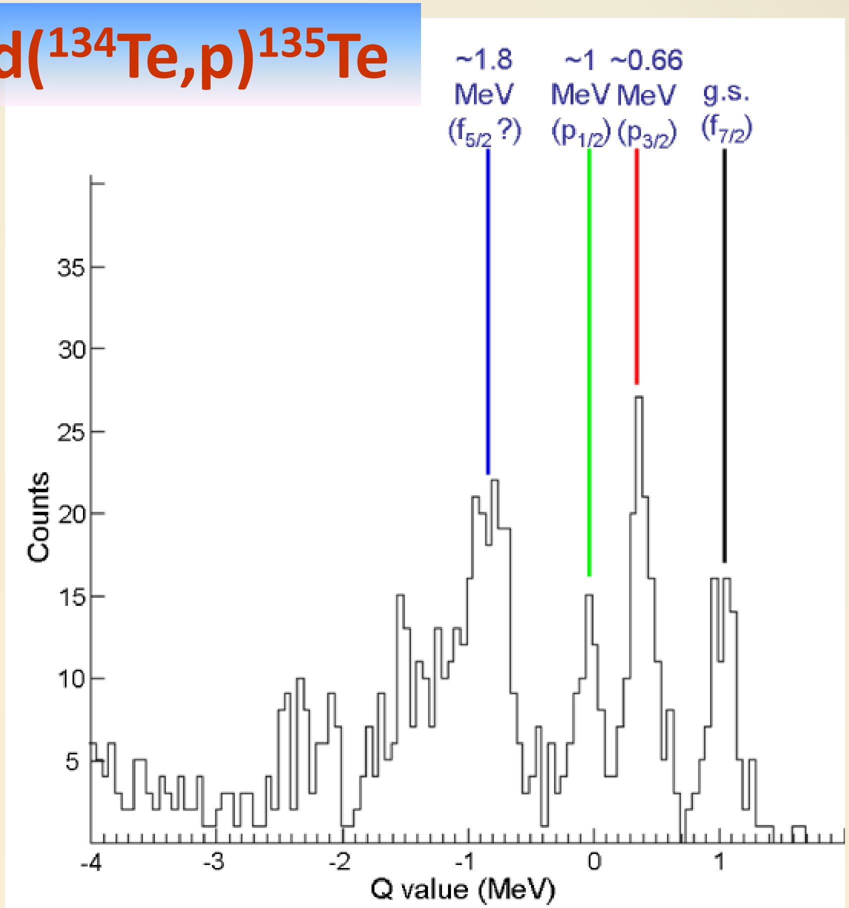

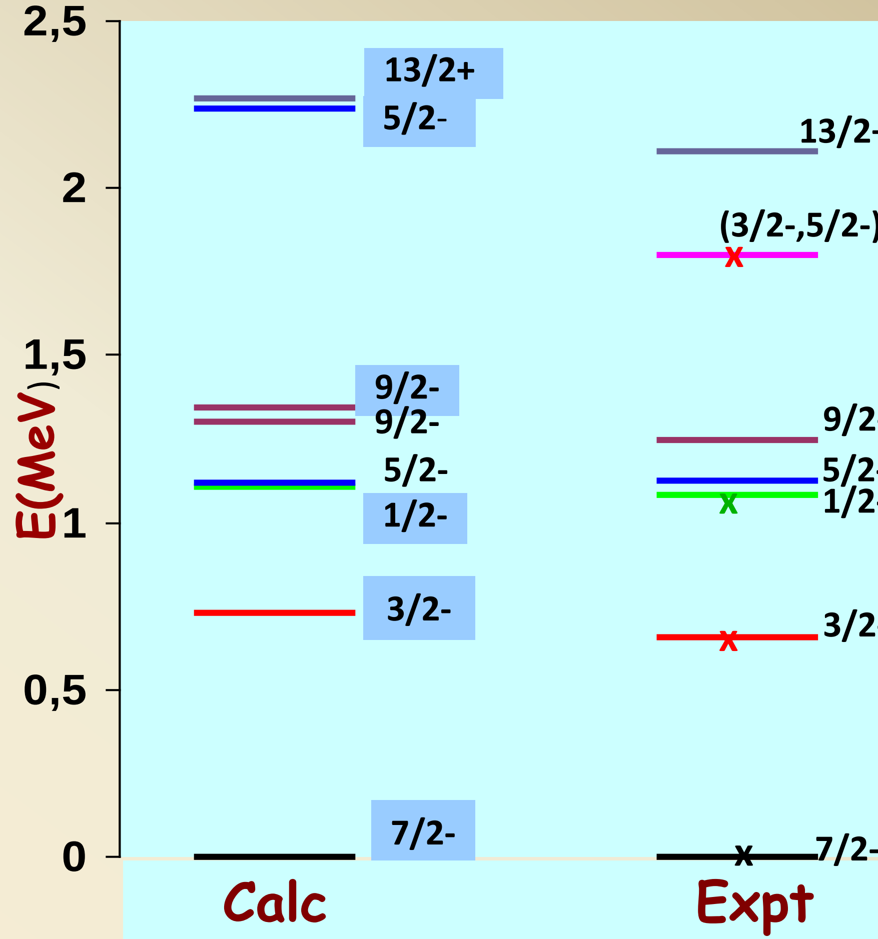

	Adopted [a] Ex (MeV)	Adopted [a] J^π	Preliminary Results [b] Ex (MeV)	Preliminary Results [b] ℓ transfer	Preliminary Results [b] J^π
^{135}Te[c]	0.000	(7/2$^-$)	0.0	(3)	(7/2$^-$)
S_n=3.34 MeV	0.659	(3/2$^-$)	≈0.66	(1)	(3/2$^-$)
	1.083	(1/2$^-$)	≈1.00	(1)	(1/2$^-$)
	1.837	(3/2$^-$,5/2$^-$)	≈1.80		

3/2-		5/2-	
E(MeV)	S	E(MeV)	S
1.72	0.27	1.62	0.00
1.81	0.00	1.71	0.00
2.23	0.05	1.82	0.06
		2.01	0.06

Summary

- Realistic shell-model calculations are a reliable tool for shell structure studies ➔
  its predictions may stimulate and be helpful to future experiments

- A lot of data are still missing in ^{132}**Sn**, for "**exotic**" as well as for "**less exotic" nuclei**. Present facilities can still produce interesting measurements,
  but with the future RIBs facilities a further step cn be done towards a better comphension of nucler structure

- The new data will be of **key importance to constrain nuclear model**
  to clarify the concept of mean field, shell structure,
  to investigate the relevant features of the effective interactions and their connections with the "bare" potential

LOI@SPES

B. Melon	Coulomb-Excitation Measurements of Radioactive Ions (^{134}Sn,^{136}Te,…)
R. Lozeva	Nuclear Moment Studies with Galileo (^{129,131}In, ^{134}Sn, ^{134}Te,…)
B. Szpak	Structure of Sb Nuclei around 132Sn as a Testing Ground for Realistic Shell Model Interactions (^{132,134}Sb)
S. Mengoni	Direct Reactions with SPES Beams: Nuclear Magicity at Z~50 N~82 … (^{123,131,133,134}Sn,^{131}In, ^{133}Sb)
G. Rainovsky	Study of Quadrupole Isovector Valence-Shell Excitations of Exotic Nuclei at SPES (^{138}Xe, ^{140}Ba, ^{132,136}Te, ^{128,132}Cd)